



**HAL**  
open science

## A specific molecular signature in SARS-CoV-2 infected kidney biopsies

Pierre Isnard, Paul Vergnaud, Serge Garbay, Matthieu Jamme, Maeva Eloudzeri, Alexandre Karras, Dany Anglicheau, Valerie Galantine, Arwa Jalal Eddine, Clément Gosset, et al.

### ► To cite this version:

Pierre Isnard, Paul Vergnaud, Serge Garbay, Matthieu Jamme, Maeva Eloudzeri, et al.. A specific molecular signature in SARS-CoV-2 infected kidney biopsies. JCI Insight, In press, pp.e165192. 10.1172/jci.insight.165192 . pasteur-04004769

**HAL Id: pasteur-04004769**

**<https://pasteur.hal.science/pasteur-04004769>**

Submitted on 25 Feb 2023

**HAL** is a multi-disciplinary open access archive for the deposit and dissemination of scientific research documents, whether they are published or not. The documents may come from teaching and research institutions in France or abroad, or from public or private research centers.

L'archive ouverte pluridisciplinaire **HAL**, est destinée au dépôt et à la diffusion de documents scientifiques de niveau recherche, publiés ou non, émanant des établissements d'enseignement et de recherche français ou étrangers, des laboratoires publics ou privés.



Distributed under a Creative Commons Attribution 4.0 International License

## A specific molecular signature in SARS-CoV-2 infected kidney biopsies

Pierre Isnard, ... , Fabiola Terzi, Marion Rabant

*JCI Insight*. 2023. <https://doi.org/10.1172/jci.insight.165192>.

Research In-Press Preview COVID-19 Nephrology

Acute kidney injury (AKI) is one of the most important complications in COVID-19 patients and is considered a negative prognostic factor with respect to patient survival. The occurrence of direct infection of the kidney by SARS-CoV-2, and its contribution to the renal deterioration process, remains a controversial issue. By studying 32 renal biopsies from COVID-19 patients we confirmed that the major pathological feature of COVID-19 is acute tubular injury (ATI). Using smFISH, we showed that the SARS-CoV-2 infects living renal cells and that infection, which parallels renal ACE2 expression levels, is associated to increase death. Mechanistically, a transcriptomic analysis uncovered specific molecular signatures in SARS-CoV-2 infected kidneys as compared to healthy kidneys and non-COVID-19 ATI kidneys. On the other hand, we demonstrated that SARS-CoV-2 and Hantavirus, two RNA viruses, activated different genetic networks despite they triggered the same pathological lesions. Finally, we identified XAF1 as a critical target of SARS-CoV-2 infection. In conclusion, this study demonstrates that SARS-CoV2 can directly infect living renal cells and identified specific druggable molecular targets that can potentially aid in the design of novel therapeutic strategies to preserve renal function in severely affected COVID-19 patients.

**Find the latest version:**

<https://jci.me/165192/pdf>



## A specific molecular signature in SARS-CoV-2 infected kidney biopsies

Pierre Isnard, MD<sup>1,2†</sup>, Paul Vergnaud, MD<sup>1\*</sup>, Serge Garbay, MSc<sup>1</sup>, Matthieu Jamme, MD<sup>3\*</sup>,  
Maeva Eloudzeri, MSc<sup>1</sup>, Alexandre Karras, MD, PhD<sup>4</sup>, Dany Anglicheau, MD, PhD<sup>5</sup>, Valérie  
Galantine, MD<sup>6</sup>, Arwa Jalal Eddine, MD<sup>7</sup>, Clément Gosset, MD<sup>8</sup>, Frank Pourcine, MD<sup>9</sup>,  
Mohammed Zarhrate, MSc<sup>10</sup>, Jean-Baptiste Gibier, MD<sup>11</sup>, Elena Rensen, PhD<sup>12</sup>, Stefano  
Pietropaoli, PhD<sup>13</sup>, Giovanna Barba-Spaeth, PhD<sup>13</sup>, Jean-Paul Duong-Van-Huyen, MD, PhD<sup>2</sup>,  
Thierry J Molina, MD, PhD<sup>2</sup>, Florian Mueller, PhD<sup>12</sup>, Christophe Zimmer, PhD<sup>12</sup>,  
Marco Pontoglio, PhD<sup>1\*</sup>, Fabiola Terzi, MD, PhD<sup>1\*†</sup>, Marion Rabant, MD, PhD<sup>1,2\*</sup>

\* The authors contribute equally to the work

<sup>1</sup>Université de Paris, INSERM U1151, CNRS UMR 8253, Institut Necker Enfants Malades,  
Département « Croissance et Signalisation », Paris, France

<sup>2</sup>Department of Pathology, Centre Hospitalier Universitaire Necker-Enfants Malades, APHP,  
Paris, France

<sup>3</sup>Department of Intensive Care Medicine, Centre Hospitalier Intercommunal de Poissy,  
Poissy, France

<sup>4</sup>Department of Nephrology, Centre Hospitalier Universitaire Européen Georges Pompidou,  
Paris, France

<sup>5</sup>Department of Transplantation, Centre Hospitalier Universitaire Necker-Enfants Malades,  
Paris, France

<sup>6</sup>Department of Nephrology, Centre Hospitalier Universitaire de la Guadeloupe, Pointe-à-  
Pitre, France,

<sup>7</sup>Department of Nephrology, Hôpital Foch, Paris, France

<sup>8</sup>Department of Nephrology, Centre Hospitalier Universitaire de La Réunion, Saint Denis de  
La Réunion, France

<sup>9</sup>Department of Nephrology, Centre Hospitalier de Melun, Melun, France

<sup>10</sup>Genomics Core Facility, Structure Fédérative de Recherche Necker, Université de Paris,  
Paris, France

<sup>11</sup>Department of Pathology, Centre Hospitalier Universitaire Lille, Lille, France

<sup>12</sup>Imaging and Modeling Unit, Institut Pasteur, 25 rue du Docteur Roux, 75015 Paris, France

<sup>13</sup>Structural Virology Unit, Institut Pasteur, 25 rue du Docteur Roux, 75015 Paris, France

### † Corresponding authors

Fabiola Terzi / Pierre Isnard : Université de Paris, INSERM U1151, CNRS UMR 8253,  
Institut Necker Enfants Malades, Département « Croissance  
et Signalisation »  
Faculté de Médecine Necker  
156-160 rue de Vaugirard  
75015 Paris, France  
E-mail: [fabiola.terzi@inserm.fr](mailto:fabiola.terzi@inserm.fr)  
E-mail: [pierre.isnard@inserm.fr](mailto:pierre.isnard@inserm.fr)

## **ABSTRACT**

Acute kidney injury (AKI) is one of the most important complications in COVID-19 patients and is considered a negative prognostic factor with respect to patient survival. The occurrence of direct infection of the kidney by SARS-CoV-2, and its contribution to the renal deterioration process, remains a controversial issue. By studying 32 renal biopsies from COVID-19 patients we confirmed that the major pathological feature of COVID-19 is acute tubular injury (ATI). Using smFISH, we showed that the SARS-CoV-2 infects living renal cells and that infection, which parallels renal ACE2 expression levels, is associated to increase death. Mechanistically, a transcriptomic analysis uncovered specific molecular signatures in SARS-CoV-2 infected kidneys as compared to healthy kidneys and non- COVID-19 ATI kidneys. On the other hand, we demonstrated that SARS-CoV-2 and Hantavirus, two RNA viruses, activated different genetic networks despite they triggered the same pathological lesions. Finally, we identified XAF1 as a critical target of SARS-CoV-2 infection. In conclusion, this study demonstrates that SARS-CoV2 can directly infect living renal cells and identified specific druggable molecular targets that can potentially aid in the design of novel therapeutic strategies to preserve renal function in severely affected COVID- 19 patients.

## INTRODUCTION

Coronavirus disease 2019 (COVID-19) is a recently discovered  $\beta$ -subtype coronavirus infection due to severe acute respiratory syndrome coronavirus type 2 (SARS-CoV-2) (1). COVID-19 has enormous health, economic and social impacts, resulting in a major global public issue. In the majority of cases, patients exhibit mild symptoms. However, in more severe cases, patients present an acute respiratory disease with interstitial and alveolar pneumonia which can lead to respiratory failure requiring mechanical ventilation (2). Acute kidney injury (AKI) is one of the most important complications in COVID-19 patients, occurring in almost 10% of all cases and around 50% among hospitalized patients (3–6). Despite improved knowledge and patient management, which has led to a significant reduction in mortality after the first epidemic wave, AKI remains a major complication in COVID-19 patients (7). More importantly, AKI is considered a negative prognostic factor with respect to disease severity and patient survival (6, 8, 9). COVID-19 patients also frequently present biological evidence of renal dysfunction such as proteinuria, hematuria and/or manifestations of proximal tubule impairment (3, 10–12).

Anatomo-pathological studies revealed that COVID-19-associated kidney disease results in two major morphological findings: acute tubular injury (ATI) and collapsing glomerulopathy (CG) (13, 14). CG has emerged as a distinct pathology and appears to affect mainly patients of African ancestry who have a high-risk *APOLI* genotype (15, 16).

Several potential mechanisms have been proposed to explain COVID-19-associated kidney disease, including direct cytokine or complement-mediated injury, coagulopathy, endothelial cell dysfunction and ischemic/hypoxic processes (17–19). However, the precise pathophysiology mechanisms leading to kidney lesions are not yet elucidated. Thus, there is an urgent need to uncover the molecular pathways underlying these pathological changes to develop preventive strategies.

Currently, it is still controversial whether SARS-CoV-2 can directly infect the kidney (20). Although a recent publication has shown a direct SARS-CoV-2 infection of kidney epithelial cells (21), several other studies argue against this result (13, 22–26). For example, May et al have recently failed to detect direct viral infection using immunohistochemistry in a large series of 240 native kidneys and 44 allografts (27). Along these lines, the identification of viral particles by electron microscopy (EM) or immunohistochemistry has been challenged (28–30). Indeed, viral particles may be confused with normal cell organelles such as clathrin-coated vesicles or multivesicular bodies in EM. On the other hand, the absence of appropriate negative controls prevents any definitive conclusion in the immunohistochemical studies. On the other hand, the presence of viral particles in kidney and other organs using *in situ* hybridization has been mainly shown in autopsic material. However, in this context, we cannot exclude that the multiorgan failure and severe SARS-CoV-2 infection in patients prior to death may favor virus diffusion, raising the question of whether SARS-CoV-2 may really infect living renal cells and trigger lesions.

Here, we used cutting-edge technologies to characterize the pathophysiology of kidney injury in a unique large kidney biopsy series of living SARS-CoV-2-infected patients collected at the time of kidney damage including patients under mechanical ventilation in intensive care unit. From March 2020 to March 2021, we prospectively enrolled 32 consecutive COVID-19 patients. Our results confirm the three main pathological changes most frequently reported in kidneys and identified a new morphological entity. In addition, we clearly show SARS-CoV-2 infects living renal cells and that this infection correlates with the level of angiotensin-converting enzyme 2 (ACE2), the cellular receptor for SARS-CoV-2 entry. More importantly, we identified specific molecular signatures in SARS-CoV-2 infected kidneys that may provide a basis for the development of targeted therapeutic strategies.

## RESULTS

### Clinical characteristics

The demographic characteristics, clinical and biological data of the 32 COVID-19 patients and controls are provided in **Table 1**, **Table S1**, **Table S2**, **Table S3** and **Supplemental Fig. 1A**. Briefly, patients had a mean age of 56 years (range, 4–83 years) and the majority were males (sex ratio, 2.6). Twenty-eight patients underwent native kidney biopsies, and 4 had allograft specimens. Frequent and notable comorbidities included diabetes (7 patients, 22%), obesity (6 patients, 19%), high blood pressure (19 patients, 59%) and chronic kidney disease (8 patients, 25%). SARS-CoV-2 infection was confirmed by RT-PCR for 29 patients, and SARS-CoV2 antibodies were detected in 3 unvaccinated patients. Twenty-four patients (75%) had COVID-19 pneumonia, including 14 patients (44%) with a severe form requiring mechanical ventilation. Twenty-six patients (81%) displayed acute kidney injury (AKI) of which 16 (50%) required dialysis. The other indication for renal biopsy was the appearance of proteinuria in 6 patients (19%). The delay between the onset of COVID-19 and renal biopsy was on average 28 days (range, 3-87 days). Eight patients eventually died (25%) from multiorgan failure.

### Renal morphological findings

A careful morphological analysis of kidney biopsies (**Fig. S1** and **Table S4**) revealed three main patterns of kidney-associated COVID-19 disease: acute tubular injury (ATI) in 14 patients (44%; **Fig. S1B**), collapsing glomerulopathy (CG) with ATI in 10 patients (31%; **Fig. S1C**) and thrombotic microangiopathy with C3 glomerulonephritis (TMA-C3GN) in 4 patients (12.5%; **Fig. S1D**). Other pathological features included diabetic nephropathy or focal segmental glomerulosclerosis with severe interstitial fibrosis in 4 patients (12.5%).

Pure ATI lesions were mainly observed in patients with more severe COVID-19 (**Table 1**, **Fig. S1A**) and were histologically comparable to 6 non COVID-19 ATI except for more

frequent polymorphonuclear cells in peritubular capillaritis in COVID-19 patients (**Table S5**). Consistent with previous reports<sup>14</sup> (15, 16), patients with combined CG and ATI were all of African ancestry and all tested patients (n=6) had an *APOLI* high-risk gene variant. Interestingly, 4 patients showed the association of features of endocapillary proliferative glomerulonephritis (GN), enriched in polynuclear cells, resembling post infectious GN, with glomerular and/or arteriolar TMA (**Fig. S1D, Table S6 and S7**). Of note, subepithelial humps were observed in only one patient (patient 26). Importantly, complement C3 and/or C4 serum levels were decreased in three of the four patients, suggesting an activation of the complement pathway.

### **SARS-CoV-2 infects kidney cells**

To definitively determine if SARS-CoV-2 infects renal cells, we took advantage of a sensitive single molecule fluorescence in situ hybridization (smFISH) technique designed to specifically detect SARS-CoV-2 RNA (CoronaFISH) and applied it to our 32 COVID-19 patients and control samples. We detected strong signals characterized by intense cytoplasmic perinuclear dots in formalin-fixed paraffin-embedded (FFPE) SARS-CoV-2 infected Vero cells and in lung tissue from COVID-19 patients. On the other hand, we did not detect any signal in control FFPE uninfected Vero-cells, normal lung tissue, normal kidney tissue and non-COVID-19 ATI kidneys, confirming the specificity of the CoronaFISH approach (**Fig. 1A and B**). CoronaFISH revealed that SARS-CoV-2 RNA was present in kidneys of 16 COVID-19 patients (50%) (**Fig. 1B and C**). The viral RNA was always detected in tubular cells; in some tubules, all cells were positive, whereas in others, only few cells were stained (**Fig. 1C**). Additionally, one patient with CG lesions (patient 17) showed positive interstitial macrophage-like cells and another (patient 22) revealed positive podocyte-like glomerular cells (**Fig. 1C**). Interestingly, SARS-CoV-2 RNA was detected mainly in kidneys from patients with severe COVID-19 disease and pure ATI lesions (11 patients, 78%, **Table S4**).

Moreover, we also detected viral RNA in 5 CG-ATI patients (50%). It is worth noting that we could not detect any viral RNA in TMA/C3GN patients and in the “other lesions” group (**Table S4**). There was no difference in the delay of renal biopsy between Corona FISH- positive and Corona FISH-negative patients (31 days (range: 3-77 days) compared to 24 days (range: 8-59 days) respectively). However, the mortality rate was significantly higher in COVID-19 patients with SARS-CoV-2-infected kidney (50% vs 7%, **Table S8**). Together these results show that SARS-CoV-2 can infect renal cells in living patients, and that the presence of the virus in renal tubular cells may aggravate the evolution of kidney damage. We next verified viral infection of kidney epithelial cells at the protein level, by performing immunohistochemical staining for the SARS-CoV-2 nucleocapsid protein. As expected, we could not detect any signal in control FFPE uninfected Vero-cells, normal lung and kidney tissue, whereas a strong signal was present in FFPE SARS-CoV-2 infected Vero cells and in lung tissue from COVID-19 patients (**Fig. S2A**). Similarly, kidney tissue from COVID-19 patients were positive for capsid staining. However, kidneys from non-COVID-19 patients with ATI also displayed similar tubular patterns (**Fig. S2B and C**). Together these data suggest that damaged renal tubules may express antigens that mimic SARS-CoV-2 antigens, making the specificity of SARS-CoV-2 antibodies questionable.

#### **ACE-2 expression levels correlate with renal SARS-CoV-2 infection**

It is known that ACE2, the receptor of SARS-CoV-2, is mostly expressed in renal epithelial cells (31–33). Hence, we examined the ACE2 expression pattern in our SARS-CoV-2- positive and -negative kidneys. We first confirmed that ACE2 was mainly expressed in cortical tubular cells and, to a lesser extent, in glomerular cells (parietal epithelial cells and podocytes) (**Fig. S3A**). Remarkably, we observed that ACE2 expression was significantly increased in kidneys from FISH-positive COVID-19 patients (n=9) as compared to FISH- negative COVID-19 patients (n=10) ( $P < 0.05$ ). (**Fig. S3B**). These results suggest that

differences in ACE2 levels may predict the increased susceptibility of SARS-CoV-2 infection in the kidneys of COVID-19 patients.

### **SARS-CoV-2 renal infection elicits a specific molecular signature**

In order to identify genetic networks that trigger the development of renal lesions during COVID-19, we performed RNA-seq on damaged kidneys from 9 COVID-19 patients, among which 4 were positive for SARS-CoV-2 RNA (FISH-positive) and 5 were negative (FISH-negative). Compared to 6 control healthy control kidneys, we found 785 differentially expressed genes (DEG) in COVID-19 samples (**Fig. S4**). Principal component analysis (PCA) of the top 500 most variable genes demonstrated that gene expression differences can be driven by two main components (**Fig. 2A**). The main predictor of renal gene expression was COVID-19 status, and the second predictor was the presence of renal SARS-CoV-2 RNA, with a sharp separation between FISH-positive and FISH-negative kidneys. Of interest, the analysis of DEG has identified several (K-means) clusters of genes that revealed a peculiar specific pattern underlying the FISH positivity status of kidneys. In particular, the comparison of FISH positive versus FISH-negative kidneys revealed an increase expression of specific gene clusters related to immune response pathways and cell-extracellular matrix interactions (**Fig. 2B and 2C**).

In order to determine the most relevant pathways modulated by COVID-19, we performed a gene-set enrichment analysis (GSEA) using the “hallmark” gene set (**Fig. 2D**). A significant number of genes related to inflammation, such as interferon gamma and alpha responses, TNFA, IL6 and IL2 pathways, inflammatory response and allograft rejection were highly enriched in COVID-19 kidneys compared to healthy controls. Consistent with the pathogenesis of COVID-19, complement and apoptosis pathways were also specifically enriched in COVID-19 kidneys. A significant number of genes related to the G2/M cell-cycle checkpoint was also upregulated in COVID-19 kidneys.

We next asked whether this molecular signature is specific to COVID-19 or is a common feature of kidney injury. Towards this aim, we compared the renal transcriptomic data of COVID-19 patients with those of 6 non-COVID-19 ATI patients to avoid bias due to morphological differences and to focus only on viral status in the kidney. PCA confirmed that gene expression was influenced by the presence of renal epithelial SARS-CoV-2 mRNA infection (**Fig. S5**). Moreover, K-means analysis showed a different pattern of gene expression in FISH-positive kidneys as compared to both FISH-negative and non-COVID-19 ATI kidneys. In particular, interferon alpha and gamma response pathway (cluster 2) and cell- extracellular matrix interaction (cluster 3) were specifically enriched in FISH-positive kidneys (**Fig. 3A and 3B**). To further confirmed the specific enrichment of interferon pathways in FISH-positive kidney, we compared GSEA between FISH-positive kidneys and non-COVID- 19 ATI kidneys, since that the histological lesions were comparable between these groups of patients. Interestingly, GSEA identified the interferon alpha pathway as the highest enriched gene set (NES: 1.85) in FISH-positive kidneys as compared to non-COVID-19 ATI kidneys (**Fig. 3C**). Together these data suggest that the activation of the interferon alpha pathway, a major event in innate antiviral immunity, may be used as a prognostic marker of direct renal viral infection.

To verify whether these molecular signatures are specifically triggered by SARS-CoV-2 or is a general feature of virus kidney infection, we performed RNA-seq on Hantavirus damaged kidney. The old-world Hantavirus (*Orthohantavirus puumala*) is an RNA virus with renal tropism that leads to the same renal lesions as COVID-19, including ATI and microvascular inflammation (34). Our results showed that the renal transcriptome of these patients tends to segregate FISH-positive kidneys from Hantavirus kidneys (**Fig. S6**). Moreover, K-means analysis revealed a particular strong enrichment of immune response pathways in Hantavirus kidneys compared to healthy kidneys (**Fig. 4A**). In a similar way, fibrotic and proliferative

pathways were particularly enriched in SARS-CoV-2-infected kidneys (**Fig. 4B**). GSEA showed that several pathways including oxidative phosphorylation, Myc targets or protein secretion are strongly induced in Hantavirus compared to FISH-positive kidneys (**Fig. S7**). Finally, we compared only kidneys with the same lesion pattern, i.e. FISH-positive, Hantavirus damaged and non-COVID-19 ATI kidneys. Interestingly, PCA uncovered that gene expression was significantly different between Hantavirus and SARS-CoV-2 infected kidneys (**Fig. S8**). Consistently, K-means revealed specific immune pathway enrichment in Hantavirus damaged kidney with an unexpected strong neutrophil activation signature (**Fig. S9**). Altogether these findings reveal that the infection of different virus leads to specific signatures, despite a similar pattern of lesions.

#### **XAF1: a critical target of renal SARS-CoV-2**

Finally, we performed a volcano plot analysis to identify the specific genetic targets of SARS-CoV-2 infection. A large number of genes were significantly up- or down-regulated between COVID-19 FISH-positive patients and non-COVID-19 ATI patients. Nevertheless, only two genes were highly specifically overexpressed in FISH-positive kidneys: H3C1 (H3 Clustered Histone 1) and X-linked inhibitor of apoptosis (XIAP)-associated factor 1 (XAF1, **Fig. 5A**). Since XAF1 has been previously shown to be upregulated in inflammatory cells and epithelial lung cells infected with SARS-CoV-2 RNA (35, 36), we examined this target further. Quantitative m-RNA expression level confirmed that XAF1 was selectively upregulated in COVID-19 FISH-positive kidneys compared to non-COVID-19 ATI injured kidney and Hantavirus-infected kidneys supporting its specific upregulation in SARS-CoV-2-infected kidneys. (**Fig. 5B**). XAF1 is a tumor suppressor protein involved in cellular apoptosis, a cellular process known to participate in kidney damage during AKI. Consistently, caspase 3 staining revealed an increase in cell apoptosis in FISH-positive kidneys compared to healthy controls (**Fig. 5C**). Moreover, GSEA showed an enrichment in apoptotic genes in FISH-

positive kidneys compared to control kidneys (**Fig. 5D**), supporting the potential role of apoptosis in SARS-CoV-2-induced renal lesions.

## DISCUSSION

AKI is one of the most important complications in COVID-19 patients and is considered a negative prognostic factor with respect to patient survival. Although a number of studies have investigated the pathophysiology of AKI during COVID-19, the majority of these studies were conducted on autopsies, raising the question of the relevance of these results for living renal cells. In this study, we used cutting-edge technologies to characterize the pathophysiology of kidney injury in a unique large kidney biopsy series of living SARS-CoV-2-infected patients collected at the time of kidney damage including patients under mechanical ventilation in intensive care unit. The overarching aim was to capture the renal molecular signatures of COVID-19 and correlate them with SARS-CoV-2 infection. Our results confirmed that the major pathological feature of COVID-19 is ATI, which was associated with collapsing glomerulopathy in patients with *APOL1* high-risk gene variants. We also identified a novel pathological morphological entity characterized by the combination of thrombotic microangiopathy with C3 glomerulonephritis. Moreover, using appropriate controls, we clearly showed that SARS-CoV-2 infects living renal cells and that viral presence is associated with higher ACE2 protein expression. More importantly, transcriptomic analysis identified specific molecular signatures in SARS-CoV-2-positive kidneys, opening new therapeutic options to prevent one of the most severe complications of COVID-19.

ATI is the most frequent pathological lesion observed in patients with COVID-19-associated kidney disease. Our results indicate that these lesions were comparable to those observed in non-COVID-19 associated ATI, except for the presence of neutrophilic capillaritis. Neutrophils and neutrophil extracellular traps, two key actors of innate immunity, have emerged as a defining feature of severe COVID-19, at least in post-mortem lung tissue (37, 38). Interestingly, we also observed a massive neutrophil infiltration in a new pathological

entity discovered here: thrombotic microangiopathy with C3 glomerulonephritis (TMA-C3GN). Even if TMA as well as C3GN have been previously reported in COVID-19 patients, this is the first time, to the best of our knowledge, that these three morphological lesions have been simultaneously observed in the kidney. It is worth noting that neutrophils, endothelial cells dysfunction, coagulation dysfunction and complement activation have been reported to contribute to the severe forms of COVID-19 (17, 19, 37).

Direct infection of SARS-CoV-2 in kidneys and its contribution to lesion development remains a controversial issue. Several technical limitations prevent any clear conclusion. For example, RT-PCR, one of the most used methods to detect SARS-CoV-2 in the kidney, cannot distinguish whether viral nucleic acids are present in the blood, urines, inflammatory infiltrating or parenchymal cells (39). On the other hand, since the majority of the studies were conducted on autopsic kidneys (39), it is not clear whether SARS-CoV-2 can directly infect living renal cells. More importantly, immunohistochemistry does not seem appropriate to detect a specific SARS-CoV-2 nucleocapsid protein signal. Using appropriate controls, we clearly showed that the same exact immunoreactivity was observed in kidneys from COVID-19 and non-COVID-19 patients with ATI, suggesting that damaged renal tubules may express antigens that cross-react with anti SARS-CoV-2 specific antibodies. Similarly, May *et al* failed to clearly detect SARS-CoV-2 nucleocapsid protein in a large series of 240 biopsies (27). In fact, if she could find a positive signal in 10 over the 235 biopsies, SARS-CoV-2 mRNA experiments did not confirm this finding, suggesting a non-specific staining. Altogether these data raise concern about the specificity of SARS-CoV-2 antibodies. Using the robust technique of CoronaFISH, we provide the first clear demonstration that SARS-CoV-2 infects renal cells. Owing to the use of 96 fluorophore-conjugated probes, CoronaFISH allows sensitive and specific visualization of the viral RNA in tissues at the single cell level (40). Our study shows that SARS-CoV-2 targeted tubular cells. Since these

cells are the most damaged in kidneys of severely affected COVID-19 patients, it is tempting to speculate that such infections may aggravate the extent of kidney damage. Consistently, the prevalence of severe ATI lesions and death was higher in FISH-positive patients compared to FISH-negative. In favor of this idea, it has been also observed that SARS-CoV-2 infection aggravates epithelial damage in the lung of COVID-19 patients (41).

ACE2, the receptor of SARS-CoV-2, is expressed in renal tubular cells (31–33). Remarkably, we observed that ACE2 expression was increased in SARS-CoV-2-positive kidneys as compared to SARS-CoV-2-negative kidneys suggesting that higher receptor levels might favor viral infection. Conversely, other teams have shown that ACE2 expression decreases during coronavirus infection in lung (42, 43). If the increased expression of ACE2 in SARS-CoV-2-infected kidneys precedes tubular epithelial infection or is a direct or indirect consequence of it remain to be studied.

A major aim of our study was to define the molecular signatures of kidneys from COVID-19 patients. Compared to healthy controls, we found that a significant number of genes related to inflammation, such as interferon gamma and alpha responses, TNFA and IL6 pathways, were highly enriched in COVID-19 kidneys. Although these molecular signatures have already been reported in the blood, lung or airways (44, 45), our study provides the first evidence that these mechanisms play a role in renal deterioration upon COVID-19. Interestingly, we observed that the molecular signatures in SARS-CoV-2- and Hantavirus-damaged kidneys were significantly different despite a similar pattern of lesions. This further supports the idea that SARS-CoV-2 triggers a particular pattern of responses. Moreover, when we compared the expression profile of SARS-CoV-2-positive kidneys with non-COVID-19 ATI kidneys, we observed a strong activation of the interferon alpha pathway. Anti-cytokines and anti-interferon therapies in COVID-19 critical illness has been extensively discussed (46). Our

data suggest that the same therapies might be beneficial in protecting the kidney from SARS-CoV-2-induced lesions.

Another molecular signature that may deserve particular attention is the G2/M cell-cycle checkpoint, which was strongly activated in SARS-CoV-2-positive kidneys as compared to non-COVID-19 ATI kidneys. Interestingly, a G2/M arrest has been shown to favor renal fibrosis after renal ischemia (47). Consistently, Jansen et al. have shown that COVID-19 patients present tubulo-interstitial fibrosis and that SARS-CoV-2 infection stimulates profibrotic signaling in human kidney organoids (48). Whether this molecular signature predicts the development of chronic kidney disease in patients with SARS-CoV-2-positive kidneys is a risk factor that deserves to be monitored in long-term follow-up studies.

We also found the *XAF1* gene was specifically upregulated in SARS-CoV-2-positive kidney biopsies compared to controls, SARS-CoV-2-negative COVID-19 kidneys and Hantavirus-infected kidneys. *XAF1* has been reported to be a highly and specific enriched gene in SARS-CoV2-infected lung epithelial and immune cells (35, 36). *XAF1* is a tumor suppressor gene known to trigger apoptosis by counteracting the inhibitory effect of IAP proteins family that in turn inhibit caspases (49). Of interest, *XAF1* has been shown to drive apoptosis of T cells in COVID-19 patients (35). The observation that apoptosis was increased in SARS-CoV2-infected kidneys and that apoptotic genes were enriched in the same tissue suggest a potential mechanistic role of *XAF1* in renal tubular damage. Interestingly, apoptosis has been also shown to be increased in renal tubular epithelial cells in a mouse model (k18-hACE2 mice) of severe COVID-19 (50), reinforcing the possible role of programmed cell death in the pathophysiology of renal injury during SARS-CoV-2 infection. However, we cannot formally exclude that *XAF1* is simply a biomarker of SARS-COV-2 kidney infection. Further studies are required to demonstrate the possible mechanistic involvement of *XAF1* in SARS-CoV-2- induced epithelial apoptosis.

We acknowledge that this work has two main limitations. First, the number of patients. However, we provide a unique cohort of living patients whose kidney samples were collected at the early time of SARS-CoV-2 infection, including patients with severe COVID-19 in intensive care units. Second, the quality of RNA. The degree of RNA degradation is inevitably related to this clinical context. In fact, the kidney biopsies were initially performed for a diagnostic purpose and, therefore, kidney samples were not optimized for RNA preservation. To compensate this limitation, we used specific tools adapted to the degraded RNA for the constitution of the RNAseq libraries (Ovation Universal RNA-Seq System) and performed “loess correction” in order to compensate for the difference in RNA integrity.

The relative lack of knowledge of the pathophysiology of kidney disease in COVID-19 patients and associated controversial information have limited our ability to develop kidney- targeted therapeutic strategies able to treat and maybe prevent this severe life-threatening complication. By expanding the pathophysiological and molecular insights on the virus- kidney interplay in the setting of COVID-19, our study provides a solid background to design and test new candidate drugs to prevent renal failure in severely affected COVID-19 patients.

## **METHODS**

### **Study design and patients**

From March 2020 to March 2021, we prospectively enrolled 32 consecutive COVID-19 patients who underwent kidney biopsy 1-3 days from the onset of acute kidney injury and/or proteinuria in 7 French hospitals: Hôpital Européen Georges Pompidou (Paris, France), Centre Hospitalier Intercommunal de Poissy (Poissy, France), Centre Hospitalier Universitaire de la Guadeloupe (Pointe-à-Pitre, France), Hôpital Foch (Paris, France), Centre Hospitalier Universitaire de La Réunion (Saint Denis de La Réunion, France), Centre Hospitalier de Melun (Melun, France) and Hôpital Necker-Enfants Malades (Paris, France). Clinical and biological data available at kidney biopsy were collected. In the majority of cases, 2 cores of renal biopsies were obtained by percutaneous biopsies, one for light microscopy and the other for immunofluorescence and molecular studies. Lung autopsy material from one COVID-19 patient was provided by the human biological sample bank of the Lille COVID working group "LICORN" (Lille, France). Kidney and lung material from control patients originated from our Pathology Department at Necker-Enfants Malades Hospital (Paris, France). In total, we studied as controls: 6 patients with normal kidney histology (healthy controls), 6 patients with ATI prior to the COVID-19 pandemic, 4 patients with Hantavirus associated kidney lesions (Hôpital Necker-Enfants Malades, Paris, France and CHU Lille, Lille, France) and 1 patient with normal lung histology. Healthy controls were individuals that were subjected to kidney biopsy because of a low-rate proteinuria ( $< 1$  g/l) or mild hematuria, with no microscopic abnormalities nor immunofluorescent deposits. ATI control group was matched according to the degree of kidney ATI lesions. Demographic data of healthy kidneys control group are provided in **Supplemental Table S1**. Clinical, biological and pathological findings of the Hantavirus control group are provided in **Supplemental Table S2**.

The protocol was approved by the Institutional Review Board of Necker Hospital, and informed written consent was obtained from all patients.

### **Histological analysis**

Kidney biopsies were fixed in formalin, alcohol and acetic acid and paraffin embedded. Four- $\mu$ m sections were stained with hematoxylin-eosin, periodic acid–Schiff, Masson trichrome, and methenamine silver. Renal lesions were blindly examined by 2 different pathologists. Lesion quantifications were made according to the Banff Classification of Renal Allograft Pathology (2018) for interstitial inflammation; tubulitis; peritubular capillaritis; interstitial fibrosis; tubular atrophy; fibrous intimal thickening; and arteriolar hyalinosis (51). Interstitial edema and ATI being a more often diffuse lesion process was evaluated as: absent (0), mild (1) or severe (2) .

### **Immunohistochemistry and Immunofluorescence**

For immunohistochemistry (IHC), an automated IHC stainer BOND-III (Leica Biosystems) was used. Briefly, 4- $\mu$ m sections of paraffin-embedded kidneys were submitted for appropriate antigen retrieval. Then, sections were incubated with the following antibodies: rabbit monoclonal anti-ACE2 antibody (Abcam, 1:100), rabbit monoclonal anti-cleaved caspase 3 antibody (Cell signaling, 1:200), rabbit polyclonal anti-recombinant nucleoprotein from SARS-CoV antibody (a gift from Nicolas Escriou, Institut Pasteur, Paris, France), rabbit polyclonal SARS-CoV-2 anti-nucleoprotein (Novusbio, 1:500). ACE2 expression was evaluated by image quantification using the “Integrated Density” program of ImageJ software on whole kidney sections (X200). This measurement integrates the product of area and the mean intensity value above a specific threshold. This estimates the amount of the strength of the expression of a specific epitope.

Immunofluorescence was performed on frozen kidney biopsies using antibodies targeting the heavy chains of immunoglobulins (IgA, IgG, IgM), kappa and lambda light chains,

complement (C3, C1q) and fibrinogen using the automated stainer BOND-III (Leica Biosystems). Immunofluorescence staining was performed on 26 of the 32 biopsies.

### **Vero cells and infection of cell lines**

Control and SARS-Cov-2 infected Vero cells originated from BetaCoV/France/IDF0372/2020. For IHC and fluorescence in situ hybridization (FISH) validation on formalin-fixed paraffin-embedded samples, paraffin-embedded control and infected Vero cell suspensions were prepared using the Cytoblock Cell Block Preparation System (Thermo Scientific) according to the manufacturer's instructions.

### **RNA-FISH**

To visualize viral RNA (vRNA) molecules from SARS-CoV2, we used the single molecule FISH (smFISH) approach as previously described and validated (52). Briefly, 96 unlabeled primary probes were designed to specifically target the positive stranded SARS-CoV-2 RNA, and were pre-hybridized with fluorescently labeled secondary detector oligonucleotides for visualization (Cy5, 647). Images were acquired with a Spinning Disk Confocal Microscope (Yokogawa CSU-X1, Zeiss Axio-Observer Z1).

### **APOL1 genotyping**

Six of the ten patients with CG lesions based on kidney biopsy underwent *APOL1* genetic analysis using DNA extracted from peripheral blood. The search for SNPs (single nucleotide polymorphisms) defining the risk variants of the *APOL1* gene was done by real-time PCR genotyping with allelic discrimination (QuantStudio 7 Flex Real-Time PCR System; Applied Biosystems®, ThermoFisher Scientific). The probes were used to identify the following SNPs: s73885319 (p.S342G) and rs60910145 (p.I384M) for the G1 variant, and the indel rs71785313 (p.NYK388K) for the G2 variant.

## **RNA-sequencing**

Transcriptomic analysis was performed on 21 native kidney biopsies: 12 control kidneys (6 normal healthy kidneys and 6 non-COVID-19 kidneys with ATI) and 9 COVID-19-associated kidney disease kidneys, of which 4 were FISH-positive (SARS-CoV-2 infected kidneys) and 5 were FISH-negative (uninfected kidneys). mRNA was extracted from nitrogen-frozen and Optimal Cutting Temperature (OCT) embedded kidneys using the miRNeasy Kit (QIAGEN) according to the manufacturer's instructions. The quantity and integrity of the purified RNA were assessed using the nanodrop spectrophotometer ND-1000 (Thermo Fisher Scientific) and capillary electrophoresis (Agilent) for RNA integrity number (RIN).

Preparation of RNA sample libraries and RNA sequencing was performed by the Genomics Core Laboratory at Imagine Institute (Paris, France). Renal biopsies were originally frozen embedded in OCT for immunofluorescence studies. This processing, which is not optimized for RNA preservation, inevitably led to a certain degree of RNA degradation. To compensate for this, the "Ovation Universal RNA-Seq System" (Nugen, Tecan) was used to prepare the RNAseq libraries. After a preliminary DNase digestion with a thermosensitive DNase (Arcticzyme), total RNA was reverse transcribed and a second strand of cDNA was synthesized. A fragmentation step was performed (or skipped for the most degraded total RNA samples) before Illumina-compatible indexed adaptor ligation. The ligation was followed by strand-selection enzymatic reactions to keep the information about the orientation of the transcripts. Insert Dependent Adaptor Cleavage (InDA-C) reactions were performed to deplete all cDNA corresponding to human ribosomal transcripts before PCR enrichment. To ensure that no excessive amplification was performed during the final PCR step, the number of PCR cycles applied to each sample was evaluated in a preliminary qPCR test using EvaGreen. An equimolar pool of final indexed RNA-Seq libraries was sequenced on the

Illumina NovaSeq6000 (100 base paired-end reads) and ~50 million paired-end reads per library were produced.

### **RNA-sequencing analysis and statistics**

The quality of reads was assessed using FastQC and aligned to the GRCh38 human reference genome with HISAT2. Gene expression was quantified by htseq-count (version 0.13.5). Given the observed level of RNA degradation, we inspected the RNA integrity using RSeqC (<https://sourceforge.net/projects/rseqc>) (53). Only samples with a median OR and average “Transcript Integrity Number” (TIN) >30 were considered and subsequently adjusted using “loess correction” in order to compensate for the difference in RNA integrity (53). Among the 17 native COVID-19 kidney biopsies available for RNA extraction, 8 had fully degraded RNA (RIN < 1.5 and TIN <30) and were not used for RNA sequencing analysis. The mean RIN and TIN of the 21 analyzed samples (COVID-19 and control) were respectively  $6.6 \pm 2.4$  and  $51 \pm 6.7$ .

Differential expression was calculated with EdgeR and lists of differentially expressed genes were generated by applying a two-fold change cut off and P-value with Benjamini-Hochberg False Discovery Rate (FDR) multiple testings ( $P < 0.05$ ) correction. Gene expression profile analyses (principal component analysis and Venn diagram) were performed using R version 4.1.1. K-means gene expression clustering was performed using ComplexHeatmap\_2.8.0 on R. Cluster profiling from K-means was performed using clusterProfiler\_4.0.5 on R. When no cluster profiles were identified using clusterProfiler\_4.0.5, cluster profiling was performed with EnrichR (<https://maayanlab.cloud/Enrichr/>) using GESA Hallmark gene set.

As the RNA-seq analysis of the Hantavirus control group was performed later in another batch, to allow accurate differential expression evaluations between groups we have re-sequenced the healthy, non-COVID-19 ATI and FISH-positive kidneys groups and performed

batch effect adjustment for RNA-seq count data using ComBat-seq (<https://academic.oup.com/nargab/article/2/3/lqaa078/5909519>) (54).

Gene Set Enrichment Analysis (GSEA version 4.1.0) was used to evaluate the transcriptional profiles between groups as previously described (<https://www.gsea-msigdb.org/gsea/index.jsp>).

RNA-seq data for all samples have been deposited in the Gene Expression Omnibus (GSE202182).

### **Statistics**

Clinical and biological data are expressed as means (quantitative variables) or ratio (categorical variables). Differences between groups were evaluated using either one-way ANOVA followed by, when significant ( $P < 0.05$ ), the Tukey-Kramer test for quantitative variables or Fisher's exact test for qualitative variables. Statistical analyses were performed using GraphPad Prism.

## **ACKNOWLEDGMENTS**

We are grateful to Christine Bole (genomics platform, Imagine, Paris) for the RNA-seq experiments. We thank Nicolas Escriou (Innovation Laboratory: Vaccines, Institut Pasteur, Paris, France) for providing the SARS-CoV antibodies. We thank Nicolas Kuperwasser for critical advice. This work was supported by Université Paris Cité, INSERM, AP-HP, Société Française de Néphrologie, Dialyse et Transplantation, Fondation Total.

## **AUTHOR CONTRIBUTION**

PI, MR: conception of the study, acquisition, analysis and interpretation of the data, wrote the manuscript; PV, MJ, ME, SG, VG, AJE, CG, FP, MZ, ER, SP, JBG: acquisition and analysis of the data, edition of the manuscript; AK, JPDVH, TM, FM, CZ, GBS: analysis and interpretation of the data, edition of the manuscript; MP, FT: conception of the study, analysis and interpretation of the data, wrote the manuscript. PI, MR, MJ VG, AJE, CG, FP, AK, DA, JPDVH: took care of the reported patients.

All the authors facilitated the study and declare they have seen and approved the final version of the manuscript.

## **DISCLOSURE**

Authors have disclosed no conflicts of interest.

## REFERENCES

1. Gorbalenya AE, et al. The species Severe acute respiratory syndrome-related coronavirus: classifying 2019-nCoV and naming it SARS-CoV-2. *Nat. Microbiol.* 2020;5(March). doi:10.1038/s41564-020-0695-z
2. Zhu N, et al. A novel coronavirus from patients with pneumonia in China, 2019. *N. Engl. J. Med.* 2020;382(8):727–733.
3. Zheng X, et al. Prevalence of Kidney Injury and Associations with Critical Illness and Death in Patients with COVID-19. *Clin. J. Am. Soc. Nephrol.* 2020;CJN.04780420.
4. Chen Y, et al. Incidence of acute kidney injury in COVID- 19 infection : a systematic review and meta- analysis. *Crit. Care* 2020;1–4.
5. Chan L, et al. AKI in Hospitalized Patients with COVID-19. *J. Am. Soc. Nephrol.* 2020;ASN.2020050615.
6. Neugarten J, et al. AKI in Hospitalized Patients with and without COVID-19: A Comparison Study. *J. Am. Soc. Nephrol.* 2020;31(9):2145–2157.
7. Dellepiane S, et al. Acute Kidney Injury in Patients Hospitalized With COVID-19 in New York City: Temporal Trends From March 2020 to April 2021. *Kidney Med.* 2021;3(5):877–879.
8. Cheng Y, et al. Kidney disease is associated with in-hospital death of patients with COVID-19. *Kidney Int.* 2020;1–10.
9. Gupta S, et al. AKI Treated with Renal Replacement Therapy in Critically Ill Patients with COVID-19. *J. Am. Soc. Nephrol.* 2020;ASN.2020060897.
10. Braun F, Huber TB, Puelles VG. Proximal tubular dysfunction in patients with COVID-19: what have we learnt so far?. *Kidney Int.* 2020;98(5):1092–1094.
11. Karras A, et al. Proteinuria and Clinical Outcomes in Hospitalized COVID-19 Patients. *Clin. J. Am. Soc. Nephrol.* 2021;16(4):514–521.

12. Werion A, et al. SARS-CoV-2 causes a specific dysfunction of the kidney proximal tubule. *Kidney Int.* 2020;98(5):1296–1307.
13. Akilesh S, et al. Multicenter Clinicopathologic Correlation of Kidney Biopsies Performed in COVID-19 Patients Presenting With Acute Kidney Injury or Proteinuria. *Am. J. Kidney Dis.* 2021;77(1):82-93.e1.
14. Sharma P, et al. Pathology of COVID-19-associated acute kidney injury. *Clin. Kidney J.* 2021;14(Supplement\_1):i30–i39.
15. Velez JCQ, Caza T, Larsen CP. COVAN is the new HIVAN: the re-emergence of collapsing glomerulopathy with COVID-19. *Nat. Rev. Nephrol.* 2020;16(10):565–567.
16. Shetty AA, et al. COVID-19–Associated Glomerular Disease. *J. Am. Soc. Nephrol.* 2020;ASN.2020060804.
17. Teuwen LA, et al. COVID-19: the vasculature unleashed. *Nat. Rev. Immunol.* 2020;20(7):389–391.
18. Ramlall V, et al. Immune complement and coagulation dysfunction in adverse outcomes of SARS-CoV-2 infection. *Nat. Med.* 2020;26(10):1609–1615.
19. Java A, et al. The complement system in COVID-19: Friend and foe?. *JCI Insight* 2020;5(15):1–12.
20. Hassler L, et al. Evidence for and against direct kidney infection by SARS-CoV-2 in patients with COVID-19. *Clin. J. Am. Soc. Nephrol.* 2021;16(11):1755–1765.
21. Victor G. Puelles, M.D., Ph.D. Marc Lütgehetmann, M.D. Maja T. Lindenmeyer, Ph.D. Jan P. Sperhake, M.D. Milagros N. Wong, M.D. Lena Allweiss, Ph.D. Silvia Chilla Axel Heinemann, M.D. Nicola Wannier, Ph.D. Shuya Liu, Ph.D. Fabian Braun, M.D. Shun Lu, Ph.D. MDC. Multiorgan and Renal Tropism of SARS-CoV-2. *N. Engl. J. Med.* 2020;4–6.
22. Golmai P, et al. Histopathologic and Ultrastructural Findings in Postmortem Kidney

- Biopsy Material in 12 Patients with AKI and COVID-19. *J. Am. Soc. Nephrol.* 2020;31(9):1944–1947.
23. Sharma P, et al. COVID-19–Associated Kidney Injury: A Case Series of Kidney Biopsy Findings. *J. Am. Soc. Nephrol.* 2020;31(9):1948–1958.
  24. Santoriello D, et al. Postmortem Kidney Pathology Findings in Patients with COVID-19. *J. Am. Soc. Nephrol.* 2020;31(9):2158–2167.
  25. Xia P, et al. Clinicopathological Features and Outcomes of Acute Kidney Injury in Critically Ill COVID-19 with Prolonged Disease Course: A Retrospective Cohort. *J. Am. Soc. Nephrol.* 2020;31(9):2205–2221.
  26. Kudose S, et al. Kidney Biopsy Findings in Patients with COVID-19. *J. Am. Soc. Nephrol.* 2020;31(9):1959–1968.
  27. May RM, et al. A multi-center retrospective cohort study defines the spectrum of kidney pathology in Coronavirus 2019 Disease (COVID-19). *Kidney Int.* 2021;100(6):1303–1315.
  28. Farkash EA, Wilson AM, Jentzen JM. Ultrastructural evidence for direct renal infection with sars-cov-2. *J. Am. Soc. Nephrol.* 2020;31(8):1683–1687.
  29. Su H, et al. Renal histopathological analysis of 26 postmortem findings of patients with COVID-19 in China. *Kidney Int.* [published online ahead of print: 2020]; doi:10.1016/j.kint.2020.04.003
  30. Kissling S, et al. Collapsing glomerulopathy in a COVID-19 patient.. *Kidney Int.* [published online ahead of print: 2020]; doi:10.1016/j.kint.2020.04.006
  31. Lely AT, et al. Renal ACE2 expression in human kidney disease. *J. Pathol.* 2004;204(5):587–593.
  32. Lee JW, Chou CL, Knepper MA. Deep sequencing in microdissected renal tubules identifies nephron segment-specific transcriptomes. *J. Am. Soc. Nephrol.*

- 2015;26(11):2669–2677.
33. Ye M, et al. Glomerular localization and expression of angiotensin-converting enzyme 2 and angiotensin-converting enzyme: Implications for albuminuria in diabetes. *J. Am. Soc. Nephrol.* 2006;17(11):3067–3075.
  34. Gnemmi V, et al. Microvascular inflammation and acute tubular necrosis are major histologic features of hantavirus nephropathy. *Hum. Pathol.* 2015;46(6):827–835.
  35. Zhu L, et al. Single-Cell Sequencing of Peripheral Mononuclear Cells Reveals Distinct Immune Response Landscapes of COVID-19 and Influenza Patients. *Immunity* 2020;53(3):685-696.e3.
  36. Hachim MY, et al. Interferon-Induced Transmembrane Protein (IFITM3) Is Upregulated Explicitly in SARS-CoV-2 Infected Lung Epithelial Cells. *Front. Immunol.* 2020;11(June):1–9.
  37. Zuo Y, et al. Neutrophil extracellular traps in COVID-19. *JCI Insight* 2020;5(11). doi:10.1172/jci.insight.138999
  38. Barnes BJ, et al. Targeting potential drivers of COVID-19: Neutrophil extracellular traps. *J. Exp. Med.* 2020;217(6):1–7.
  39. Khan S, et al. Does SARS-CoV-2 Infect the Kidney?. *J. Am. Soc. Nephrol.* 2020;ASN.2020081229.
  40. Tsanov N, et al. SmiFISH and FISH-quant - A flexible single RNA detection approach with super-resolution capability. *Nucleic Acids Res.* 2016;44(22):1–11.
  41. Bhatnagar J, et al. Evidence of Severe Acute Respiratory Syndrome Coronavirus 2 Replication and Tropism in the Lungs, Airways, and Vascular Endothelium of Patients With Fatal Coronavirus Disease 2019: An Autopsy Case Series. *J. Infect. Dis.* [published online ahead of print: 2021]; doi:10.1093/infdis/jiab039
  42. Kuba K, et al. A crucial role of angiotensin converting enzyme 2 (ACE2) in SARS

- coronavirus-induced lung injury. *Nat. Med.* 2005;11(8):875–879.
43. Yamaguchi T, et al. ACE2-like carboxypeptidase B38-CAP protects from SARS-CoV-2-induced lung injury. *Nat. Commun.* 2021;12(1). doi:10.1038/s41467-021-27097-8
  44. Daamen AR, et al. Comprehensive transcriptomic analysis of COVID-19 blood, lung, and airway. *Sci. Rep.* 2021;11(1):1–19.
  45. Blanco-Melo D, et al. Imbalanced Host Response to SARS-CoV-2 Drives Development of COVID-19. *Cell* 2020;181(5):1036-1045.e9.
  46. Jamilloux Y, et al. Should we stimulate or suppress immune responses in COVID-19? Cytokine and anti-cytokine interventions. *Autoimmun. Rev.* 2020; doi:10.1016/j.autrev.2020.102567
  47. Yang L, et al. Epithelial cell cycle arrest in G2/M mediates kidney fibrosis after injury. *Nat. Med.* [published online ahead of print: 2010]; doi:10.1038/nm.2144
  48. Jansen J, et al. SARS-CoV-2 infects the human kidney and drives fibrosis in kidney organoids. *Cell Stem Cell* 2022;29(2):217-231.e8.
  49. Deveraux QL, Reed JC. IAP family proteins - Suppressors of apoptosis. *Genes Dev.* 1999;13(3):239–252.
  50. Hassler L, et al. A Novel Soluble ACE2 Protein Provides Lung and Kidney Protection in Mice Susceptible to Lethal SARS-CoV-2 Infection. *J. Am. Soc. Nephrol.* 2022;ASN.2021091209.
  51. Roufosse C, et al. A 2018 Reference Guide to the Banff Classification of Renal Allograft Pathology. *Transplantation* 2018;102(11):1795–1814.
  52. Rensen E, et al. Sensitive visualization of SARS-CoV-2 RNA with CoronaFISH. *Life Sci. Alliance* 2022;5(4):e202101124.
  53. Wang L, et al. Measure transcript integrity using RNA-seq data. *BMC Bioinformatics* 2016;1–16.

54. Zhang Y, Parmigiani G, Johnson WE. ComBat-seq: Batch effect adjustment for RNA-seq count data. *NAR Genomics Bioinforma.* 2020;2(3):1–10

**Table 1: Characteristics of COVID-19 patients**

	All patients n=32	ATI n=14	CG-ATI n=10	TMA/C3GN n=4	Other n=4	P Value
<b>Patients' demographic</b>						
Male; n (%)	23 (72%)	10 (71%)	7 (70%)	2 (50%)	4 (100%)	ns
Age; years	56 [4-83]	63 [50-77]	47 [29-69]	44 [4-68]	69 [53-83]	ns
History of CKD or renal graft; n (%)	12 (38%)	1 (7%)*	6 (60%)*	1 (25%)	4 (100%)	0.009
1 or more severe COVID-19 risk factors; n (%)	25 (78%)	10 (71%)	9 (90%)	2 (50%)	4 (100%)	ns
<b>Clinical parameters</b>						
Delay between COVID-19 onset and biopsy; day	29 [3-87]	26 [3-77]	32 [5-87]	34.3 [10-62]	23 [9-41]	ns
Interstitial pneumopathy (CT-scan); n (%)	24 (75%)	13 (93%)*	7 (70%)	1 (25%)*	3 (75%)	0.019
Oxygen therapy requirement; n (%)	20 (63%)	13 (93%)*/†	3 (30%)*	1 (25%)†	3 (75%)	0.002*/0.019†
Mechanical ventilation; n (%)	14 (44%)	12 (86%)*/‡	0 (0%)*	1 (25%)†	1 (25%)‡	<0.001*/0.044‡†
Renal replacement therapy requirement; n (%)	16 (50%)	10 (71%)*	1 (10%)*	2 (50%)	3 (75%)	0.004
Mortality rate; n (%)	8 (25%)	7 (50%)*	0 (0%)*	(0%)	1 (25%)	0.019
<b>Biological parameters</b>						
Serum creatinine level; µmol/L	546 [55-2696]	261 [55-1363]*	948 [171-2696]*	342 [169-559]	741 [190-2092]	0.045
Blood urea nitrogen; mmol/L	25.6 [2.7-78]	9.3 [2.7-36]	104.4 [13-528]	43.5 [14-73]	51.3 [22-78]	ns
Proteinuria/creatininuria; g/mmol	0.72 [0.05-3.9]	0.59 [0.05-2.31]	0.97 [0.29-3.9]	0.43 [0.09-0.9]	0.74 [0.07-1.3]	ns
Microalbuminuria/creatininuria; mg/mmol	397 [5.8-2122]	40 [5.8-234]*/†	645 [152-2008]*	N/A	1052 [340-2122]†	0.03*/0.005†
Serum albumin level; g/L	26 [15-34]	28 [19-34]*	23 [15-33]*	N/A	27 [22-32]	0.047
C-reactive protein; mg/L	101 [1.6-369]	155 [46-369]*	23.8 [1.6-93]*/†	146 [8.9-310]†	79.2 [19-186]	<0.001*/0.03†

ATI: Acute Tubular Injury; CG: Collapsing Glomerulopathy; TMA/C3GN: Thrombotic Microangiopathy/C3 Glomerulonephritis; CKD: Chronic Kidney Disease; CT-scan: Computer assisted Tomography scan. Data are expressed as the mean with range [Min-Max] unless otherwise specified. Differences between the groups were evaluated using either one-way ANOVA followed by, when significant ( $P < 0.05$ ), the Tukey-Kramer for quantitative variable or Fisher's exact test for qualitative variable. \* ‡ † indicates the 2 corresponding groups with a P value  $< 0.05$ . ns: not significant.

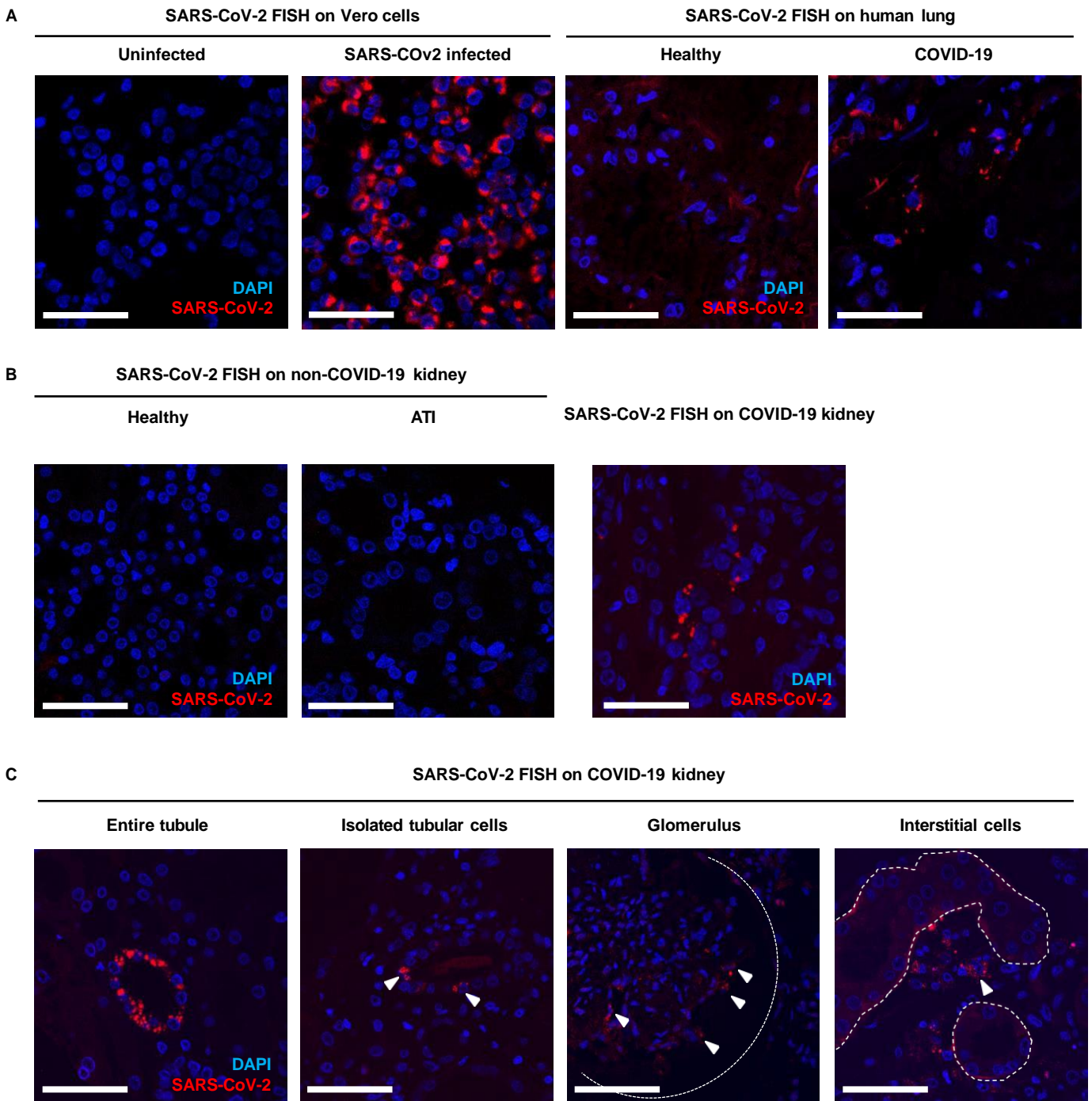


**Figure 1**

**Figure 1: SARS-CoV-2 infects kidney cells.** A: Results of SARS-CoV-2 FISH on uninfected and SARS-CoV-2-infected Vero cells (left) and on human lung tissue of healthy and COVID-19 patients (right). B: Results of SARS-CoV-2 FISH on control kidneys (healthy and ATI of non-COVID-19 patients) and on a kidney from a COVID-19 patient. C: representative images of the different patterns of SARS-CoV-2 FISH detection in kidneys from COVID-19 patients. Of note, the first two images on the left show SARS-Co-2 staining in tubules. The third image from the left, shows SARS-Co-2 staining in a glomerulus. The dotted lines underline the glomerular capsule. The fourth image (right) shows SARS-Co-2 staining in interstitial cells. The dotted lines underline the tubular basal membrane. White arrows show positive cells. Positive-strand RNA was labeled with Cy5 (red), and nuclei in blue (DAPI). Scale bars in all panels: 100  $\mu$ m.

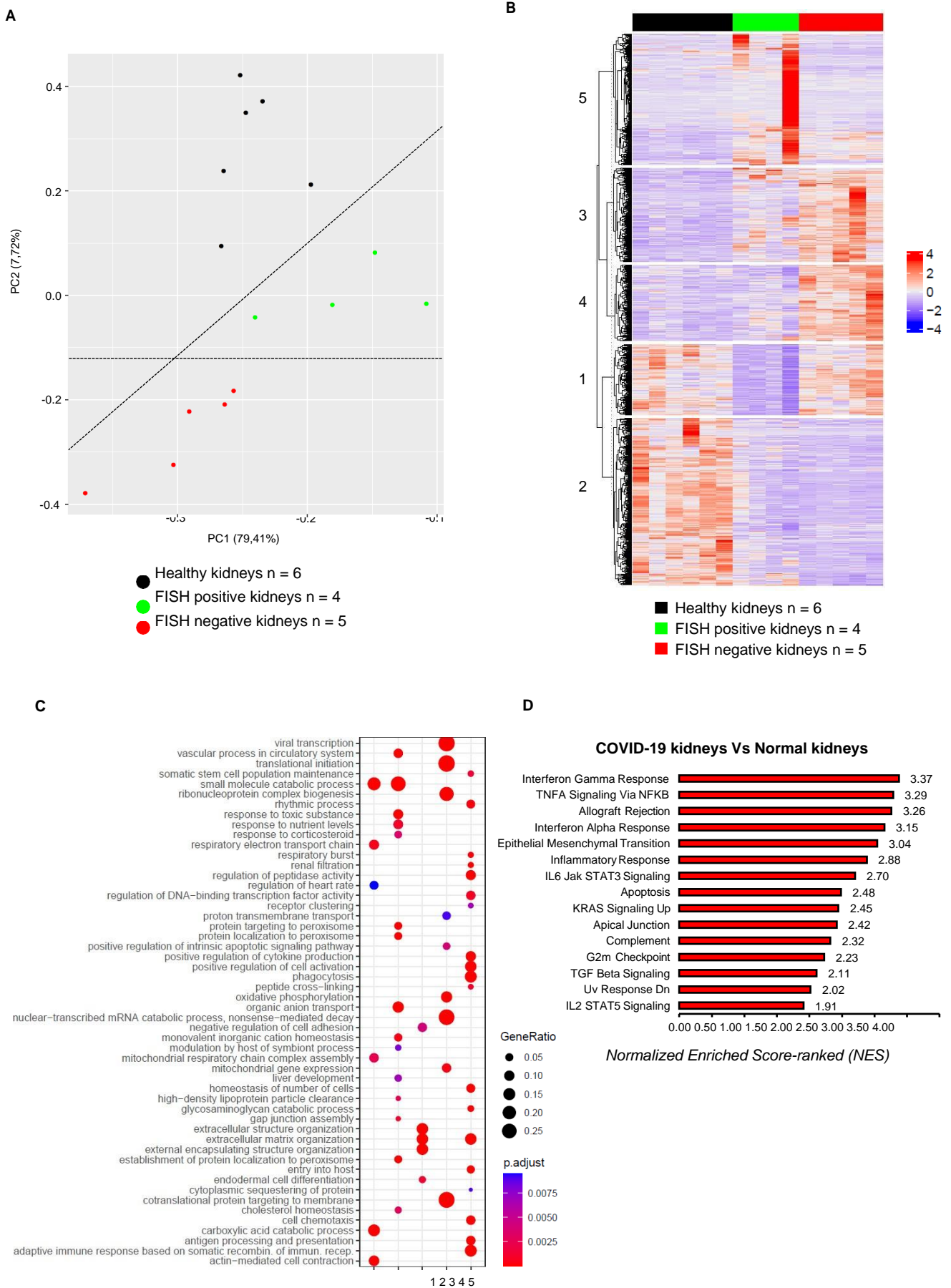


**Figure 2**

**Figure 2: SARS-CoV-2 renal infection elicits a specific molecular signature. A:** Principal component analysis (PCA) of the top 500 most variable genes in SARS-COV-2 FISH positive and FISH negative kidneys and healthy kidneys. **B:** Heat map representing K-means analysis of differentially expressed genes comparing healthy kidneys, SARS-COV-2 FISH-positive and SARS-COV-2 FISH-negative COVID-19 kidneys. **C:** Dot plot of the cluster profiling analysis from K-means comparing healthy kidneys, SARS-COV-2 FISH-positive and SARS- COV-2 FISH-negative COVID-19 kidneys. **D:** Bar plot of the top 15 normalized enriched score-ranked gene sets (Hallmark, GSEA) with  $q < 0.001$  in COVID-19 kidneys compared to healthy kidneys.

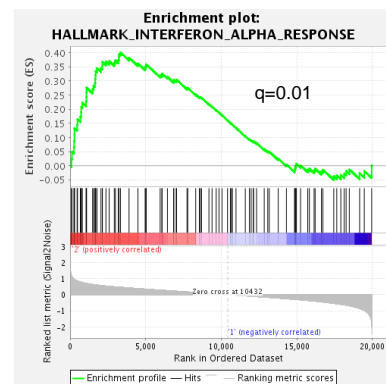
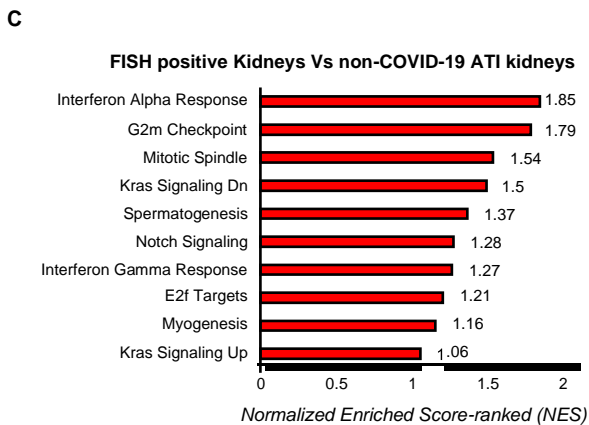
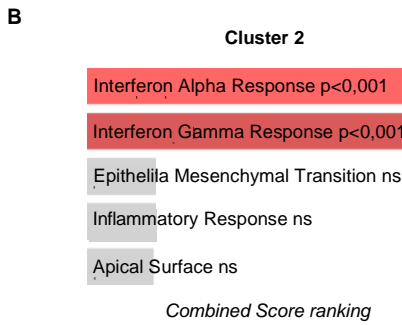
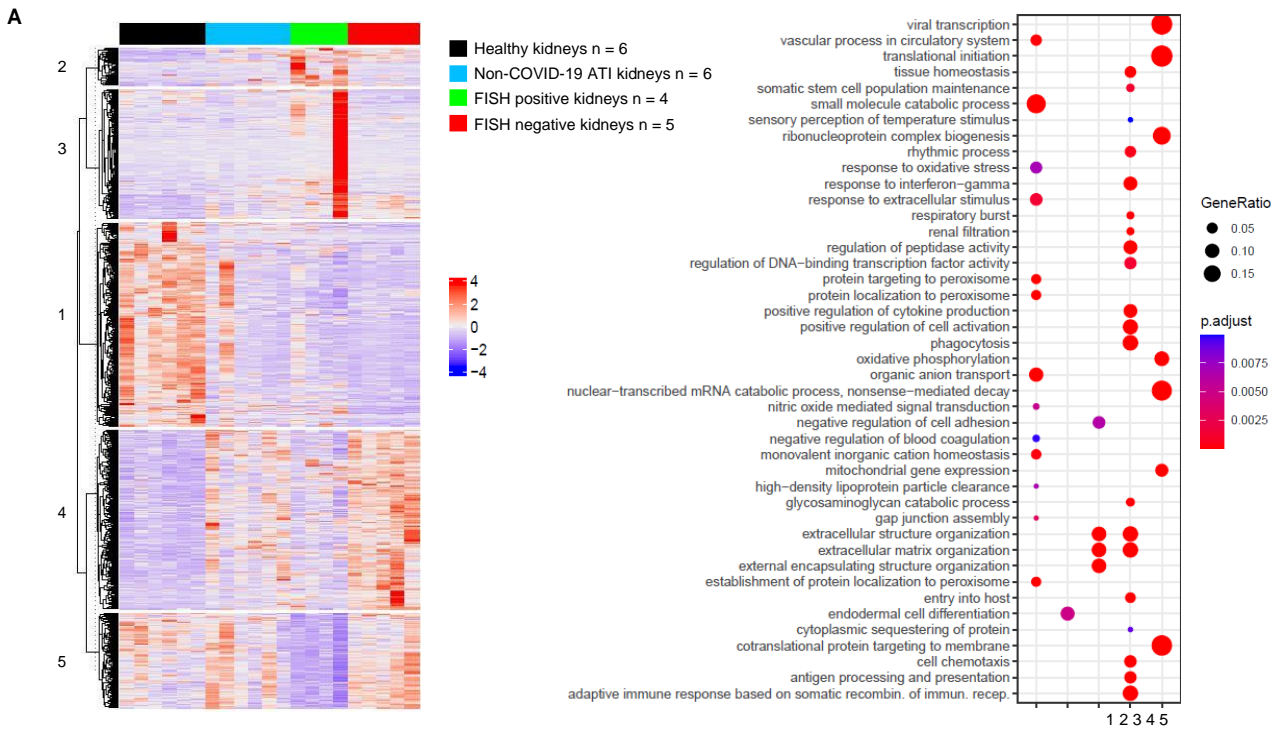


**Figure 3**

**Figure 3: SARS-CoV-2 renal infection elicits a specific molecular signature compared to non-COVID-19 ATI kidneys.** **A:** Heat map representing K-means analysis with the corresponding dot plot of the cluster profiling of differentially expressed genes comparing healthy kidneys, SARS-CoV-2 FISH-positive, SARS-CoV-2 FISH-negative and non-COVID-19 ATI kidneys. **B:** Bar plot of the top five combined score-ranked gene set (Hallmark, GSEA) from cluster 2 of the K-means clustering analysis comparing healthy kidneys, SARS- CoV-2 FISH-positive, SARS-CoV-2 FISH-negative and non-COVID-19 ATI kidneys. **C:** Bar plot of the top ten normalized enriched score-ranked gene set (Hallmark, GSEA) of FISH- positive COVID-19 kidneys compared to non-COVID-19 ATI kidneys (left panel). Hallmark interferon alpha enrichment plot from GSEA analysis comparing FISH-positive COVID-19 kidneys to non-COVID-19 ATI kidneys (right panel).

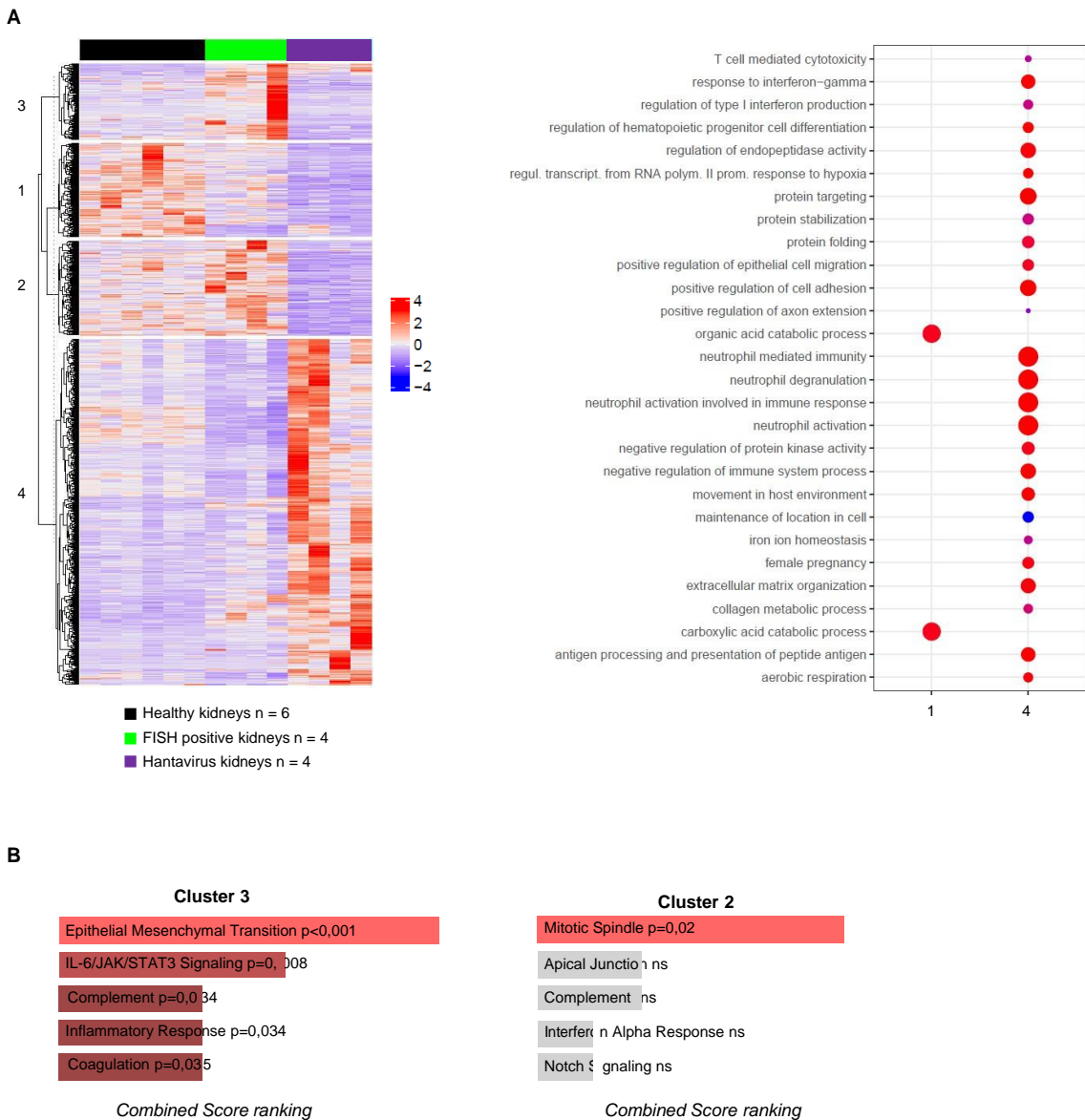
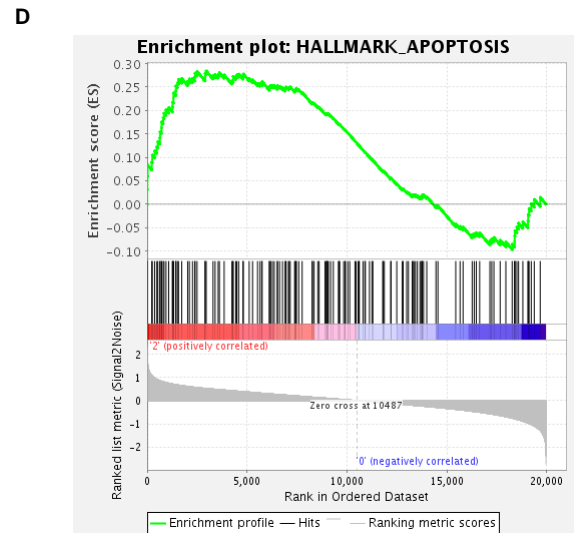
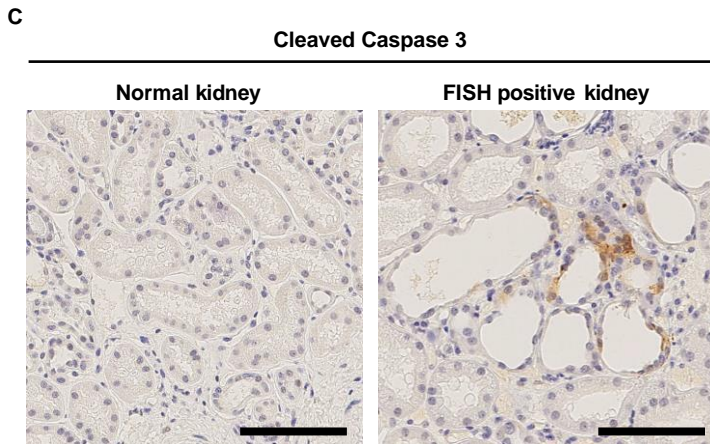
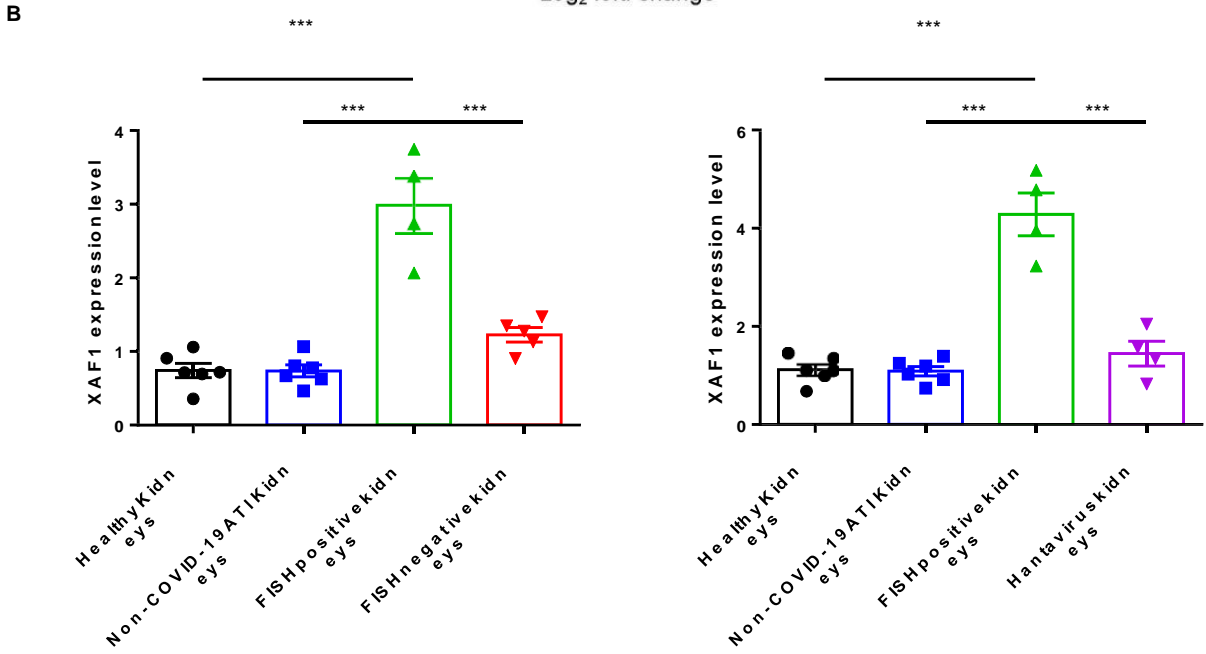
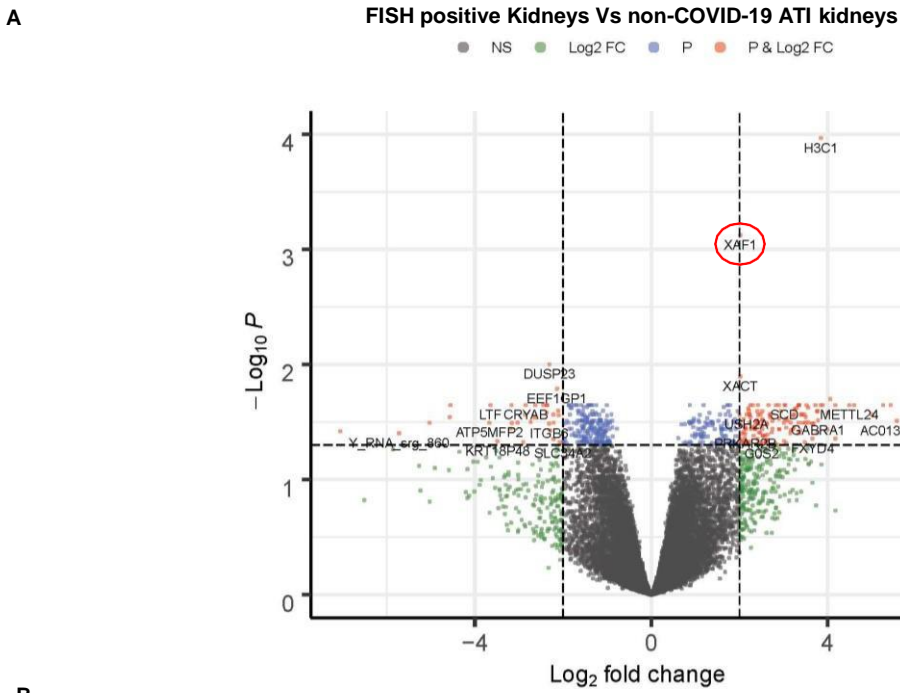


**Figure 4**

**Figure 4: SARS-CoV-2 renal infection elicits a specific molecular signature compared to Hantavirus kidneys**

**A:** Heat map representing K-means analysis with the corresponding dot plot of the cluster profiling of differentially expressed genes comparing healthy kidneys, SARS-COV-2 FISH- positive and Hantavirus kidneys. **B:** Bar plot of the top five combined score-ranked gene set (Hallmark, GSEA) from cluster 2 and 3 of the K-means clustering analysis comparing healthy kidneys, SARS-COV-2 FISH-positive and Hantavirus kidneys.



**FISH positive kidneys Vs Normal kidneys**

**Figure 5**

**Figure 5: XAF1 is a critical target of renal SARS-CoV-2.** **A:** Volcano plot of differentially expressed genes comparing FISH-positive COVID-19 kidneys to non-COVID-19 ATI kidneys. **B:** Comparative XAF1 gene expression in healthy kidneys, non-COVID-19 ATI kidneys, FISH-positive and FISH-negative COVID-19 kidneys (left panel) and healthy kidneys, non-COVID-19 ATI kidneys, FISH-positive and Hantavirus kidneys (right panel). Tukey-Kramer test was applied to test the significance of the difference. \*\*\*  $P < 0.001$ . **C:** Representative images of cleaved caspase 3 immunostaining in healthy kidneys and FISH- positive COVID-19 kidneys. **D:** Hallmark apoptosis enrichment plot from GSEA analysis comparing FISH-positive COVID-19 kidneys to healthy controls.